Preprints of the 21st IFAC World Congress (Virtual)
Berlin, Germany, July 12-17, 2020

Trajectory Planning for a Segway Model exploiting Inherent Feedforward Structure [1]

Christian Zauner * **Andreas Müller** * **Hubert Gattringer** *
Matthias Jörgl **

* *Institute of Robotics, Johannes Kepler University Linz, Altenbergerstraße 69, 4040 Linz, Austria, (e-mail: {christian.zauner, a.mueller, hubert.gattringer}@jku.at).*
** *Trotec Laser GmbH, Freilingerstraße 99, 4614 Marchtrenk, Austria.*

Abstract: Time/energy optimal trajectory planning for a Segway model (inverted pendulum on two independently actuated wheels) is addressed. Basis for this planning is the dynamical model for this under-actuated, non-holonomic multibody system. In order to reduce the calculation effort for the optimization, an input/output transformation is applied, which leads to a control system in strict feedforward form. The full system state can thus be described by two outputs, which are parameterized by two B-splines. The system is required to move on the ground within a predefined area. For the optimization the control points of the B-Splines serve as optimization variables and the cost functional is comprised of the overall energy of the robot and the terminal time. Additionally to the maximum motor velocities and torques, the maximum ground reaction forces give rise to the constraints. The latter are crucial to ensure that the wheels do not slip.

Keywords: Motion Control Systems, Mobile Robots, Modeling, Feedback Linearization, Trajectory and Path Planning

1. INTRODUCTION

Segway-type mobile systems have attracted attention not only for leisure activities but also for logistic applications. Since this under-actuated non-holonomic mechanism, is inherently unstable, the use of model-based control is crucial for reliable operation. There exist quite a number of contributions addressing the derivation of the nonlinear dynamic model, e.g. Ghaffari et al. (2016) focuses on the effect of the nonlinear coupling terms, and the control of such a system. Without any claim to completeness a few of them are listed here. The linear control problem is addressed in Salerno and Angeles (2004), Kim et al. (2005) and Albert et al. (2018), while various nonlinear control algorithms are examined in Pathak et al. (2005), Cui et al. (2015) and Kim and Kwon (2017). Worth mentioning is, that in Albert et al. (2018) structure-preserving trajectory optimization is performed using variational integrators. In this paper time/energy-optimal motion planning of the Segway model in Fig. 1 is addressed using a direct approach to optimal control. Since it has so far not been possible to find a flat output for the Segway model, which would substantially simplify this task (Levine (2009)), a partial feedback linearization (Isidori (1995)) is applied. It is shown that the resulting system has a strict feedforward structure. The latter allows expressing the system trajectory in terms of the outputs of the associated transformed system. In contrast to differentially flat systems, the strict feedforward structure involves a cascaded integration chain to deduce the state from the outputs. To the best of our knowledge no effort has been made so far to exploit this special structure in order to reduce the calculation effort while optimizing trajectories. The chosen two outputs (heading and rolling angle) are described with B-splines. The optimal control problem then becomes a constrained optimization problem in terms of the B-spline parameters. Constraints account for the geometric bounds of the area the Segway is allowed to move and for the limits on velocity and motor torques.

[1] This work has been supported by the "LCM - K2 Center for Symbiotic Mechatronics" within the framework of the Austrian COMET-K2 program.

2. MATHEMATICAL MODELING

2.1 Dynamic Model

In order to describe the dynamic behavior of the Segway model, consisting of 3 rigid bodies, shown in Fig. 1, the equations of motion are needed. Therefore the generalized coordinates $\mathbf{q} = (x\ y\ \gamma\ \theta\ \xi\ \eta)^\intercal$ are introduced, with the position x, y and the orientation γ in the horizontal plane, the inclination angle θ of the basis, and the relative rotation angles ξ and η of the wheels. Since ideal rolling of the wheels is assumed, non-holonomic constraints (constraints at velocity level) have to be considered. This leads to the kinematic relation $\dot{\mathbf{q}} = \mathbf{H}(\gamma)\dot{\mathbf{s}}$ with the matrix

$$\mathbf{H}(\gamma) = \begin{bmatrix} \cos(\gamma) & 0 & 0 \\ \sin(\gamma) & 0 & 0 \\ 0 & 1 & 0 \\ 0 & 0 & 1 \\ \frac{2}{D_W} & -\frac{2a_W}{D_W} & -1 \\ \frac{2}{D_W} & \frac{2a_W}{D_W} & -1 \end{bmatrix} \tag{1}$$

and the vector of minimal velocities $\dot{\mathbf{s}} = \begin{pmatrix} v_L & \dot{\gamma} & \dot{\theta} \end{pmatrix}^\intercal$, with the longitudinal velocity v_L and the angular velocities $\dot{\gamma}$ and $\dot{\theta}$. The dimensions a_W and D_W are indicated in Fig. 1.

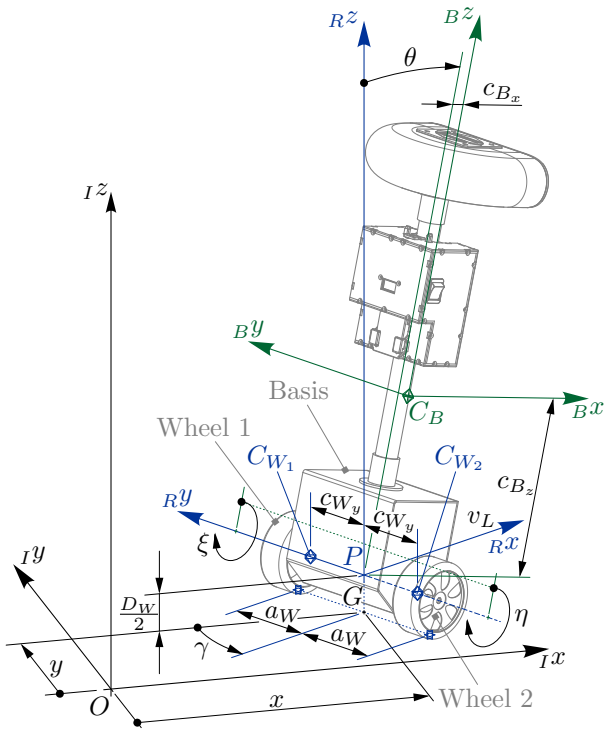

Fig. 1. Segway with reference frames, minimal coordinates and important dimensions

The generalized coordinates and the minimal velocities can be combined to the vector of states $\mathbf{x} = \left(\mathbf{q}^\mathsf{T}\ \dot{\mathbf{s}}^\mathsf{T}\right)^\mathsf{T}$. Likewise the driving torques can be combined to the vector of inputs $\mathbf{u} = (M_1\ M_2)^\mathsf{T}$. Furthermore the dynamic properties collected in Tab. 1 as well as the positions of the centers of gravity C_B, C_{W_1} and C_{W_2} indicated by c_{B_x}, c_{B_z} and c_{W_y} in Fig. 1 have to be considered. Using these definitions and by applying synthetic methods proposed in Bremer (2008) the equations of motion in configuration space representation

$$\mathbf{M}(\theta)\ddot{\mathbf{s}} + \mathbf{g}(\theta, \dot{\mathbf{s}}) = \mathbf{B}\mathbf{u} \tag{2}$$

can be obtained. The derivation can be found in Appendix A. The symmetric positive definite mass matrix

$$\mathbf{M}(\theta) = \begin{bmatrix} M_{1,1} & 0 & M_{1,3}(\theta) \\ 0 & M_{2,2}(\theta) & 0 \\ M_{3,1}(\theta) & 0 & M_{3,3} \end{bmatrix} \tag{3}$$

consists of the constant entries

$$M_{1,1} = m_B + 2m_W + \tfrac{8}{{D_W}^2}\left(J_{W_a} + {i_G}^2 J_M\right) \tag{4}$$

$$M_{3,3} = J_{B_y} + m_B\left({c_{B_x}}^2 + {c_{B_z}}^2\right) \tag{5}$$

and the state dependent entries

$$M_{1,3}(\theta) = M_{3,1}(\theta) = m_B\left(c_{B_z}\cos(\theta) - c_{B_x}\sin(\theta)\right) \tag{6}$$

$$\begin{aligned} M_{2,2}(\theta) = {} & J_{B_z}\cos(\theta)^2 + J_{B_x}\sin(\theta)^2 \\ & + m_B\left(c_{B_x}\cos(\theta) + c_{B_z}\sin(\theta)\right)^2 \\ & + 2\left(J_{W_r} + m_W {c_{W_y}}^2\right) + \tfrac{8{a_W}^2}{{D_W}^2}\left(J_{W_a} + {i_G}^2 J_M\right). \end{aligned} \tag{7}$$

The state dependent generalized forces are collected in the vector

$$\mathbf{g}(\theta, \dot{\mathbf{s}}) = \begin{pmatrix} g_1(\theta, \dot{\mathbf{s}}) \\ g_2(\theta, \dot{\mathbf{s}}) \\ g_3(\theta, \dot{\mathbf{s}}) \end{pmatrix} \tag{8}$$

with the entries

$$\begin{aligned} g_1(\theta, \dot{\mathbf{s}}) = {} & -\left(\dot\gamma^2 + \dot\theta^2\right) m_B\left(c_{B_x}\cos(\theta) + c_{B_z}\sin(\theta)\right) \\ & + \left(v_L\tfrac{4}{{D_W}^2} - \dot\theta\tfrac{2}{D_W}\right)(d_1 + d_2) - \dot\gamma a_W (d_1 - d_2) \end{aligned} \tag{9}$$

$$\begin{aligned} g_2(\theta, \dot{\mathbf{s}}) = {} & v_L\dot\gamma m_B\left(c_{B_x}\cos(\theta) + c_{B_z}\sin(\theta)\right) \\ & + 2\dot\gamma\dot\theta m_B c_{B_x} c_{B_z}\left(\cos(\theta)^2 - \sin(\theta)^2\right) \\ & + 2\dot\gamma\dot\theta\left(J_{B_x} + m_B {c_{B_z}}^2\right)\cos(\theta)\sin(\theta) \\ & - 2\dot\gamma\dot\theta\left(J_{B_z} + m_B {c_{B_x}}^2\right)\cos(\theta)\sin(\theta) \\ & + \dot\gamma\tfrac{4{a_W}^2}{{D_W}^2}(d_1 + d_2) + \left(\dot\theta\tfrac{2a_W}{D_W} - v_L\tfrac{4a_W}{{D_W}^2}\right)(d_1 - d_2) \end{aligned} \tag{10}$$

$$\begin{aligned} g_3(\theta, \dot{\mathbf{s}}) = {} & \dot\gamma^2 m_B c_{B_x} c_{B_z}\left(\sin(\theta)^2 - \cos(\theta)^2\right) \\ & - \dot\gamma^2\left(J_{B_x} + m_B {c_{B_z}}^2\right)\cos(\theta)\sin(\theta) \\ & + \dot\gamma^2\left(J_{B_z} + m_B {c_{B_x}}^2\right)\cos(\theta)\sin(\theta) \\ & + \left(\dot\theta - v_L\tfrac{2}{D_W}\right)(d_1 + d_2) + \dot\gamma\tfrac{2a_W}{D_W}(d_1 - d_2) \\ & - m_B g\left(c_{B_x}\cos(\theta) + c_{B_z}\sin(\theta)\right) \end{aligned} \tag{11}$$

and the constant input matrix is

$$\mathbf{B} = \begin{bmatrix} \frac{2}{D_W} & \frac{2}{D_W} \\ -\frac{2a_W}{D_W} & \frac{2a_W}{D_W} \\ -1 & -1 \end{bmatrix}. \tag{12}$$

Since the mass matrix is invertible, the equations of motion (2) can be transformed into the state space representation

$$\begin{pmatrix} \dot{\mathbf{q}} \\ \ddot{\mathbf{s}} \end{pmatrix} = \begin{pmatrix} \mathbf{H}(\gamma)\dot{\mathbf{s}} \\ -\mathbf{M}(\theta)^{-1}\mathbf{g}(\theta, \dot{\mathbf{s}}) \end{pmatrix} + \begin{bmatrix} \mathbf{0}^{6\times 2} \\ \mathbf{M}(\theta)^{-1}\mathbf{B} \end{bmatrix}\mathbf{u} \tag{13}$$

which is leading to the expression

$$\begin{aligned} \dot{\mathbf{x}} &= \mathbf{f}(\mathbf{x}) + \mathbf{G}(\mathbf{x})\mathbf{u} \\ &= \begin{pmatrix} v_L\cos(\gamma) \\ v_L\sin(\gamma) \\ \dot\gamma \\ \dot\theta \\ \frac{2}{D_W}(v_L - \dot\gamma a_W) - \dot\theta \\ \frac{2}{D_W}(v_L + \dot\gamma a_W) - \dot\theta \\ f_7(\theta, \dot{\mathbf{s}}) \\ f_8(\theta, \dot{\mathbf{s}}) \\ f_9(\theta, \dot{\mathbf{s}}) \end{pmatrix} + \begin{bmatrix} 0 & 0 \\ 0 & 0 \\ 0 & 0 \\ 0 & 0 \\ 0 & 0 \\ 0 & 0 \\ G_7(\theta) & G_7(\theta) \\ G_8(\theta) & -G_8(\theta) \\ G_9(\theta) & G_9(\theta) \end{bmatrix}\mathbf{u} \end{aligned} \tag{14}$$

with

$$f_7(\theta, \dot{\mathbf{s}}) = \tfrac{M_{1,3}(\theta)g_3(\theta,\dot{\mathbf{s}}) - M_{3,3}g_1(\theta,\dot{\mathbf{s}})}{M_{1,1}M_{3,3} - M_{1,3}(\theta)^2} \tag{15}$$

$$f_8(\theta, \dot{\mathbf{s}}) = -\tfrac{g_2(\theta,\dot{\mathbf{s}})}{M_{2,2}(\theta)} \tag{16}$$

$$f_9(\theta, \dot{\mathbf{s}}) = \tfrac{M_{1,3}(\theta)g_1(\theta,\dot{\mathbf{s}}) - M_{1,1}g_3(\theta,\dot{\mathbf{s}})}{M_{1,1}M_{3,3} - M_{1,3}(\theta)^2} \tag{17}$$

$$G_7(\theta) = \tfrac{-D_W M_{1,3}(\theta) - 2M_{3,3}}{D_W(M_{1,1}M_{3,3} - M_{1,3}(\theta)^2)} \tag{18}$$

$$G_8(\theta) = \tfrac{2a_W}{D_W M_{2,2}(\theta)} \tag{19}$$

$$G_9(\theta) = \tfrac{-D_W M_{1,1} + 2M_{1,3}(\theta)}{D_W(M_{1,1}M_{3,3} - M_{1,3}(\theta)^2)}. \tag{20}$$

Equation (14) are the (non-linear) motion equations in control-affine form, i.e. linear in the control vector.

2.2 Exact Input/Output Linearization

As the name implies the exact input/output linearization results in a linear subsystem relating a chosen (virtual) output and the resulting new inputs of the transformed system. Since there exist two inputs to the original system, two virtual outputs can be chosen. Because (3) to (11)

Table 1. Dynamic model parameters of Segway

Symbol	Description
g	gravitational acceleration
m_B	mass of basis including stators of motors
m_W	mass of a wheel including rotor of motor
J_{B_x}	moment of inertia of basis about ${}_B x$-axis
J_{B_y}	moment of inertia of basis about ${}_B y$-axis
J_{B_z}	moment of inertia of basis about ${}_B z$-axis
J_{W_a}	axial moment of inertia of a wheel (about ${}_R y$-axis)
J_{W_r}	radial moment of inertia of a wheel
J_M	axial moment of inertia of a rotor of a motor
d_1	constant of viscous friction between basis and wheel 1
d_2	constant of viscous friction between basis and wheel 2
i_G	gear box ratio

involve many trigonometric functions of θ and γ, $\mathbf{y} = (\gamma, \theta)^\intercal$ is chosen as vector of virtual outputs. Since $\mathbf{y}$ is actually put together by state coordinates of (14) its time derivatives can be easily extracted from (14) and can be stated by

$$\dot{\mathbf{y}} = \begin{pmatrix} f_3(\dot{\gamma}) \\ f_4(\dot{\theta}) \end{pmatrix} = \begin{pmatrix} \dot{\gamma} \\ \dot{\theta} \end{pmatrix} \tag{21}$$

$$\begin{aligned} \ddot{\mathbf{y}} &= \mathbf{f}_{89}(\theta, \dot{\mathbf{s}}) + \mathbf{G}_{89}(\theta)\mathbf{u} \\ &= \begin{pmatrix} f_8(\theta, \dot{\mathbf{s}}) \\ f_9(\theta, \dot{\mathbf{s}}) \end{pmatrix} + \begin{bmatrix} G_8(\theta) & -G_8(\theta) \\ G_9(\theta) & G_9(\theta) \end{bmatrix} \mathbf{u}. \end{aligned} \tag{22}$$

Since $\mathbf{G}_{89}(\theta)$ has always full rank, the linearizing state-feedback transformation can be obtained by setting $\ddot{\mathbf{y}} = \mathbf{v}$ with the new input vector $\mathbf{v}$

$$\begin{aligned} \mathbf{u} &= \mathbf{G}_{89}(\theta)^{-1} \left(\mathbf{v} - \mathbf{f}_{89}(\theta, \dot{\mathbf{s}})\right) \\ &= \begin{bmatrix} \frac{1}{2G_8(\theta)} & \frac{1}{2G_9(\theta)} \\ \frac{-1}{2G_8(\theta)} & \frac{1}{2G_9(\theta)} \end{bmatrix} \left(\mathbf{v} - \begin{pmatrix} f_8(\theta, \dot{\mathbf{s}}) \\ f_9(\theta, \dot{\mathbf{s}}) \end{pmatrix} \right). \end{aligned} \tag{23}$$

Applying this transformation to the system (14) results in

$$\begin{aligned} \dot{\mathbf{x}} &= \bar{\mathbf{f}}(\mathbf{x}) + \bar{\mathbf{G}}(\mathbf{x})\mathbf{v} \\ &= \begin{pmatrix} v_L \cos(\gamma) \\ v_L \sin(\gamma) \\ \dot{\gamma} \\ \dot{\theta} \\ \frac{2}{D_W}\left(v_L - \dot{\gamma} a_W\right) - \dot{\theta} \\ \frac{2}{D_W}\left(v_L + \dot{\gamma} a_W\right) - \dot{\theta} \\ \bar{f}_7(\theta, \dot{\gamma}, \dot{\theta}) \\ 0 \\ 0 \end{pmatrix} + \begin{bmatrix} 0 & 0 \\ 0 & 0 \\ 0 & 0 \\ 0 & 0 \\ 0 & 0 \\ 0 & 0 \\ 0 & \bar{G}_7(\theta) \\ 1 & 0 \\ 0 & 1 \end{bmatrix} \mathbf{v} \end{aligned} \tag{24}$$

with

$$\bar{f}_7(\theta, \dot{\gamma}, \dot{\theta}) = f_7(\theta, \dot{\mathbf{s}}) - \tfrac{G_7(\theta) f_9(\theta, \dot{\mathbf{s}})}{G_9(\theta)} \tag{25}$$

and

$$\bar{G}_7(\theta) = \tfrac{G_7(\theta)}{G_9(\theta)}. \tag{26}$$

It should be noted, that in equation (25) the dependency on v_L has canceled out. This is not by design, but due to the special structure of the equations of motion.

2.3 Strict Feedforward Structure

Expanding the definition of Tall and Respondek (2005) to systems with multiple affine inputs, the system

$$\dot{\boldsymbol{\zeta}} = \tilde{\mathbf{f}}(\boldsymbol{\zeta}) + \tilde{\mathbf{G}}(\boldsymbol{\zeta})\boldsymbol{\upsilon} \tag{27}$$

is in strict feedforward form, if $\tilde{\mathbf{f}}(\boldsymbol{\zeta})$ and $\tilde{\mathbf{G}}(\boldsymbol{\zeta})$ have the form

$$\tilde{\mathbf{f}}(\boldsymbol{\zeta}) = \begin{pmatrix} \tilde{f}_1(\zeta_2, \zeta_3, \ldots, \zeta_{n-1}, \zeta_n) \\ \tilde{f}_2(\zeta_3, \zeta_4, \ldots, \zeta_{n-1}, \zeta_n) \\ \vdots \\ \tilde{f}_{n-2}(\zeta_{n-1}, \zeta_n) \\ \tilde{f}_{n-1}(\zeta_n) \\ \tilde{f}_n \end{pmatrix} \tag{28}$$

and

$$\tilde{\mathbf{G}}(\boldsymbol{\zeta}) = \begin{bmatrix} \tilde{\mathbf{G}}_1(\zeta_2, \zeta_3, \ldots, \zeta_{n-1}, \zeta_n) \\ \tilde{\mathbf{G}}_2(\zeta_3, \zeta_4, \ldots, \zeta_{n-1}, \zeta_n) \\ \vdots \\ \tilde{\mathbf{G}}_{n-2}(\zeta_{n-1}, \zeta_n) \\ \tilde{\mathbf{G}}_{n-1}(\zeta_n) \\ \tilde{\mathbf{G}}_n \end{bmatrix} \tag{29}$$

respectively. This form has the advantage, that with a given input $\boldsymbol{\upsilon}$ the system state $\boldsymbol{\zeta}$ can be calculated step by step backwards from ζ_n to ζ_1 solely by integrating possibly nonlinear functions, e.g. with quadrature rules. By comparing $\bar{\mathbf{f}}(\mathbf{x})$ and $\bar{\mathbf{G}}(\mathbf{x})$ in (24) with $\tilde{\mathbf{f}}(\boldsymbol{\zeta})$ (28) and $\tilde{\mathbf{G}}(\boldsymbol{\zeta})$ (29) it can be easily seen, that rearranging the state $\mathbf{x}$ to

$$\begin{aligned} \mathbf{z} &= (z_1\ z_2\ z_3\ z_4\ z_5\ z_6\ z_7\ z_8\ z_9)^\intercal \\ &= \left(x\ y\ \xi\ \eta\ v_L\ \gamma\ \theta\ \dot{\gamma}\ \dot{\theta}\right)^\intercal \end{aligned} \tag{30}$$

leads to the system

$$\begin{aligned} \dot{\mathbf{z}} &= \bar{\tilde{\mathbf{f}}}(\mathbf{z}) + \bar{\tilde{\mathbf{G}}}(\mathbf{z})\mathbf{v} \\ &= \begin{pmatrix} z_5 \cos(z_6) \\ z_5 \sin(z_6) \\ \frac{2}{D_W}\left(z_5 - z_8 a_W\right) - z_9 \\ \frac{2}{D_W}\left(z_5 + z_8 a_W\right) - z_9 \\ \bar{f}_7(z_7, z_8, z_9) \\ z_8 \\ z_9 \\ 0 \\ 0 \end{pmatrix} + \begin{bmatrix} 0 & 0 \\ 0 & 0 \\ 0 & 0 \\ 0 & 0 \\ 0 & \bar{G}_7(z_7) \\ 0 & 0 \\ 0 & 0 \\ 1 & 0 \\ 0 & 1 \end{bmatrix} \mathbf{v}, \end{aligned} \tag{31}$$

which is already in the strict feedforward form.

2.4 Ground Reaction Forces

The reaction forces at the ground contact points G_{W_1} and G_{W_2} of the wheels are derived. The total wrench due to the two reaction forces at point G is

$$\begin{aligned} \begin{pmatrix} {}_R\mathbf{f}_G^z \\ {}_R\mathbf{M}_G^z \end{pmatrix} &= \begin{bmatrix} \mathbf{I} & \mathbf{0} \\ {}_R\tilde{\mathbf{r}}_{GC_B} & \mathbf{I} \end{bmatrix} \begin{bmatrix} \mathbf{R}_{RB} & \mathbf{0} \\ \mathbf{0} & \mathbf{R}_{RB} \end{bmatrix} \begin{pmatrix} {}_B\mathbf{f}_{C_B}^z \\ {}_B\mathbf{M}_{C_B}^z \end{pmatrix} \\ &\quad + \sum_{i=1}^{2} \begin{bmatrix} \mathbf{I} & \mathbf{0} \\ {}_R\tilde{\mathbf{r}}_{GC_{W_i}} & \mathbf{I} \end{bmatrix} \begin{pmatrix} {}_R\mathbf{f}_{C_{W_i}}^z \\ {}_R\mathbf{M}_{C_{W_i}}^z \end{pmatrix} \end{aligned} \tag{32}$$

with

$${}_R\mathbf{f}_G^z = (F_{G,x}\ F_{G,y}\ F_{G,z})^\intercal, \quad {}_R\mathbf{M}_G^z = (M_{G,x}\ M_{G,y}\ M_{G,z})^\intercal$$

$${}_R\mathbf{r}_{GC_B} = \left(0\ 0\ \tfrac{D_W}{2}\right)^\intercal + \mathbf{R}_{RB}\left(c_{B_x}\ 0\ c_{B_z}\right)^\intercal$$

$${}_R\mathbf{r}_{GC_{W_1}} = \left(0\ c_{W_y}\ \tfrac{D_W}{2}\right)^\intercal, \quad {}_R\mathbf{r}_{GC_{W_2}} = \left(0\ -c_{W_y}\ \tfrac{D_W}{2}\right)^\intercal.$$

Here $\tilde{\mathbf{r}}$ denotes the skew symmetric cross product matrix. The ${}_R x$- and ${}_R z$-components of the reaction forces at point G are separated for the two contact points of the wheels G_{W_1} and G_{W_2} by solving a linear equation system with the solution

$$\begin{pmatrix} F_{W_1,x} \\ F_{W_2,x} \\ F_{W_1,z} \\ F_{W_2,z} \end{pmatrix} = \begin{bmatrix} \frac{1}{2} & 0 & 0 & \frac{-1}{2a_W} \\ \frac{1}{2} & 0 & 0 & \frac{1}{2a_W} \\ 0 & \frac{1}{2} & \frac{1}{2a_W} & 0 \\ 0 & \frac{1}{2} & \frac{-1}{2a_W} & 0 \end{bmatrix} \begin{pmatrix} F_{G,x} \\ F_{G,z} \\ M_{G,x} \\ M_{G,z} \end{pmatrix} \tag{33}$$

Due to the collinearity of the points G, G_{W_1} and G_{W_2} the ${}_R y$-component of ${}_R\mathbf{M}_G^z$ results in $M_{G,y} = 0$. Thus the ${}_R y$-component of ${}_R\mathbf{f}_G^z$ cannot be easily separated and only the sum over the two wheels $F_{W,y} = F_{G,y}$ is relevant.

3. TRAJECTORY PLANNING

3.1 Trajectory Definition

Based on the strict feedforward formulation of the EOM a trajectory consistent with the system dynamics could be defined by two parameterized functions over time (e.g. B-splines) for $\mathbf{v}$ and integration constants for each state coordinate. On the other hand, since the linear subsystem composed of γ, θ, $\dot{\gamma}$ and $\dot{\theta}$ actually consists of two separate double integrators, it is also possible to define two B-splines of sufficiently high degree for γ and θ. Here the latter approach is chosen, because in contrast to integrating, differentiating preserves the beneficial property of the local support of the spline basis functions. In order to avoid discontinuities for the driving torques, γ and θ are defined by the B-splines of degree $n_{sp} = 3$

$$\gamma(t, \hat{\boldsymbol{\gamma}}, \hat{\mathbf{t}}) = \sum_{i=1}^{N_{sp}+n_{sp}} \hat{\gamma}_i B_i^{n_{sp}}(t, \hat{t}_i, \hat{t}_{i+1}, \dots, \hat{t}_{i+n_{sp}+1}) \tag{34}$$

and

$$\theta(t, \hat{\boldsymbol{\theta}}, \hat{\mathbf{t}}) = \sum_{i=1}^{N_{sp}+n_{sp}} \hat{\theta}_i B_i^{n_{sp}}(t, \hat{t}_i, \hat{t}_{i+1}, \dots, \hat{t}_{i+n_{sp}+1}) \tag{35}$$

with the number of spline parts N_{sp}, the i-th B-spline basis function $B_i^{n_{sp}}(t, \dots)$, where n_{sp} denotes the highest occurring degree of t, calculated by the recursive formula stated by Piegl and Tiller (2012), the vectors of control points

$$\hat{\boldsymbol{\gamma}} = \begin{pmatrix} \hat{\gamma}_1 & \hat{\gamma}_2 & \cdots & \hat{\gamma}_{N_{sp}+n_{sp}} \end{pmatrix}^\mathsf{T} \tag{36}$$

$$\hat{\boldsymbol{\theta}} = \begin{pmatrix} \hat{\theta}_1 & \hat{\theta}_2 & \cdots & \hat{\theta}_{N_{sp}+n_{sp}} \end{pmatrix}^\mathsf{T} \tag{37}$$

and the vector of knots

$$\hat{\mathbf{t}} = \begin{pmatrix} \hat{t}_1 & \hat{t}_2 & \cdots & \hat{t}_{N_{sp}+2n_{sp}+1} \end{pmatrix}^\mathsf{T} \tag{38}$$

derived from the vector of time points

$$\mathbf{t} = \begin{pmatrix} t_0 & t_1 & \cdots & t_{N_{sp}-1} & t_E \end{pmatrix}^\mathsf{T}. \tag{39}$$

Because of the knot multiplicity of $n_{sp}+1$ at the start and at the end, $\hat{t}_1 = \dots = \hat{t}_{n_{sp}+1} = t_0$ and $\hat{t}_{N_{sp}+n_{sp}+1} = \dots = \hat{t}_{N_{sp}+2n_{sp}+1} = t_E$.

Following the approach of Piegl and Tiller (2012), the needed time derivatives of the splines $\gamma(t, \hat{\boldsymbol{\gamma}}, \hat{\mathbf{t}})$ and $\theta(t, \hat{\boldsymbol{\theta}}, \hat{\mathbf{t}})$ can be calculated analytically and are again represented by splines of a reduced degree, with control points depending on $\hat{\mathbf{t}}$ and $\hat{\boldsymbol{\gamma}}$ and $\hat{\boldsymbol{\theta}}$ respectively.

The desired path on the ground surface is defined piece wise by primitive subpaths like straight lines, circular arcs and rotations. The quadratic distance measure from an accumulation of these primitives to an arbitrary point on the surface is defined by the function $\mathcal{X}(x, y)$. The valid region of positions of the point G of the Segway can be stated by the region where $\mathcal{X}(x, y) \leq \epsilon^2$ holds true, as can be seen for the example trajectory in Fig. 2.

By setting the first and last three control points to

$$\hat{\gamma}_1 = \hat{\gamma}_2 = \hat{\gamma}_3 = \gamma_0 \tag{40}$$

$$\hat{\gamma}_{N_{sp}+n_{sp}-2} = \hat{\gamma}_{N_{sp}+n_{sp}-1} = \hat{\gamma}_{N_{sp}+n_{sp}} = \gamma_E \tag{41}$$

$$\hat{\theta}_1 = \hat{\theta}_2 = \hat{\theta}_3 = \theta_e \tag{42}$$

$$\hat{\theta}_{N_{sp}+n_{sp}-2} = \hat{\theta}_{N_{sp}+n_{sp}-1} = \hat{\theta}_{N_{sp}+n_{sp}} = \theta_e \tag{43}$$

with $\theta_e = -\arctan\left(\frac{c_{B_x}}{c_{B_z}}\right)$ the trajectory is defined so to start and terminate in the upright equilibrium position. Furthermore by using x_0, y_0, γ_0, ξ_0, η_0 and $v_{L,0} = 0$ as integration constants the start state is defined by

$$\mathbf{x}_0 = \begin{pmatrix} x_0 & y_0 & \gamma_0 & \theta_e & \xi_0 & \eta_0 & 0 & 0 & 0 \end{pmatrix}^\mathsf{T}, \quad \mathbf{u}_0 = \begin{pmatrix} 0 & 0 \end{pmatrix}^\mathsf{T}. \tag{44}$$

Without loss of generality the start value for the wheel angles ξ_0 and η_0 as well as the start time t_0 is set to zero.

3.2 Trajectory Optimization

The goal is to minimize the overall required energy as well as the duration of the trajectory weighted by ν_t. Following the definitions of the previous sections the vector of optimization variables can be defined by

$$\mathbf{p} = \begin{pmatrix} \begin{pmatrix} t_1 & t_2 & \cdots & t_{N_{sp}} \end{pmatrix}^\mathsf{T} \\ \begin{pmatrix} \hat{\gamma}_4 & \hat{\gamma}_5 & \cdots & \hat{\gamma}_{N_{sp}+n_{sp}-3} \end{pmatrix}^\mathsf{T} \\ \begin{pmatrix} \hat{\theta}_4 & \hat{\theta}_5 & \cdots & \hat{\theta}_{N_{sp}+n_{sp}-3} \end{pmatrix}^\mathsf{T} \end{pmatrix}. \tag{45}$$

With these optimization variables and with the initial state of the trajectory $\mathbf{x}_0$ the time curves of the system state $\mathbf{x}(t, \mathbf{p})$, the new input $\mathbf{v}(t, \mathbf{p})$ and the driving torques $\mathbf{u}(t, \mathbf{p})$ are defined. The definition of the desired path on the ground surface gives a constraint for $x(t, \mathbf{p})$ and $y(t, \mathbf{p})$ over time and the end position defined by x_E, y_E and γ_E. An additional constraint is obtained by setting the terminal velocity $v_{L,E} = 0$. Furthermore the system limits for the motor torques as well as the motor speeds must not be exceeded. In order to exclude mathematical solutions from the outset, which contain a pendulum swing below the ground level, the inclination angle $\theta(t, \mathbf{p})$ is limited by $\theta_{max} = \frac{\pi}{4}\text{rad}$. The optimal control problem thus becomes

$$\min_{\mathbf{p}} \left(\int_{t_0}^{t_E(\mathbf{p})} \|\mathbf{u}(\tau, \mathbf{p})\|_2^2 + \nu_t \, \mathrm{d}\tau \right) \tag{46}$$

s.t.

$$\left\| \begin{pmatrix} x(t_E, \mathbf{p}) \\ y(t_E, \mathbf{p}) \end{pmatrix} - \begin{pmatrix} x_E \\ y_E \end{pmatrix} \right\|_2^2 = 0$$

$$\gamma(t_E, \mathbf{p}) - \gamma_E = 0$$

$$v_L(t_E, \mathbf{p}) = 0$$

$$\mathcal{X}(x(t, \mathbf{p}), y(t, \mathbf{p})) < \epsilon^2$$

$$|M_i(t, \mathbf{p})| < M_{max} \qquad i \in \{1, 2\}$$

$$|\dot{\xi}(t, \mathbf{p})| < \omega_{M,max}$$

$$|\dot{\eta}(t, \mathbf{p})| < \omega_{M,max}$$

$$|\theta(t, \mathbf{p})| < \theta_{max}$$

$$F_{W,z,min} < F_{W_i,z}(t, \mathbf{p}) \qquad i \in \{1, 2\}$$

$$|F_{W_i,x}(t, \mathbf{p})| < F_{W_i,x,max}(t, \mathbf{p}) \qquad i \in \{1, 2\}$$

$$|F_{W,y}(t, \mathbf{p})| < F_{W,y,max}(t, \mathbf{p})$$

with the ground reaction forces limited in such a way, that the $F_{W_i,z}(t,\mathbf{p})$ components with $i \in \{1,2\}$ are limited to a minimal compressive force and the remaining components are limited according to

$$F_{W_i,x,max}(t,\mathbf{p}) = \mu_0 F_{W_i,z}(t,\mathbf{p}) \quad i \in \{1,2\} \tag{47}$$

$$F_{W,y,max}(t,\mathbf{p}) = \sum_{i=1}^{2} \sqrt{F_{W_i,x,max}(t,\mathbf{p})^2 - F_{W_i,x}(t,\mathbf{p})^2}. \tag{48}$$

4. SIMULATION

In this section the results of the optimization of an example trajectory defined by the segments listed in Tab. 2 are shown. Since this trajectory should comply with an actually built Segway prototype as shown in Fig. 1, the model parameters and constraints are chosen according to this experimental setup. For this optimization the weight for the terminal time is set to $\nu_t = 2$. Figure 2 shows the position of the Segway on the ground surface and the region of valid positions with $\epsilon = 0.1\,\mathrm{m}$. In Fig. 3 the time curves of the relevant state coordinates are depicted. That the maximum driving torques $M_{max} = 0.705\,\mathrm{N\cdot m}$ and wheel speeds $\omega_{M,max} = 37.04\,\mathrm{rad/s}$ are not exceeded is shown in Fig. 4. Figure 5 shows that the ground reaction forces are within the cone of friction with a dry friction coefficient $\mu_0 = 0.5$ and a minimum compressive force $F_{W,z,min} = 5\,\mathrm{N}$. Thereby the rolling condition can be assumed to be satisfied. This optimization problem has been solved with an active set SQP algorithm.

Table 2. Segments of example trajectory

#	Description	Definition
-	start point	$x_0 = 0.5\,\mathrm{m}$, $y_0 = 0.5\,\mathrm{m}$, $\gamma_0 = 0\,\mathrm{rad}$
1	straight line	length: $1.5\,\mathrm{m}$
2	circular arc	radius: $0.5\,\mathrm{m}$, angle: $\pi\mathrm{rad}$
3	straight line	length: $1.3\,\mathrm{m}$
4	circular arc	radius: $0.2\,\mathrm{m}$, angle: $\frac{\pi}{2}\mathrm{rad}$
5	straight line	length: $0.8\,\mathrm{m}$
6	rotation	angle: $\frac{\pi}{2}\mathrm{rad}$
-	end point	$x_E = 0.5\,\mathrm{m}$, $y_E = 0.5\,\mathrm{m}$, $\gamma_E = 0\,\mathrm{rad}$

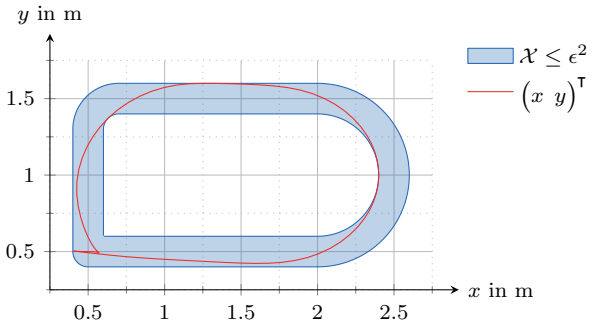

Fig. 2. Example Trajectory: Position on the surface

5. CONCLUSION

In this paper the control of a Segway (inverted pendulum on two independently actuated wheels) as a highly nonlinear control system is considered. It was shown that the control system associated to the input-output linearized

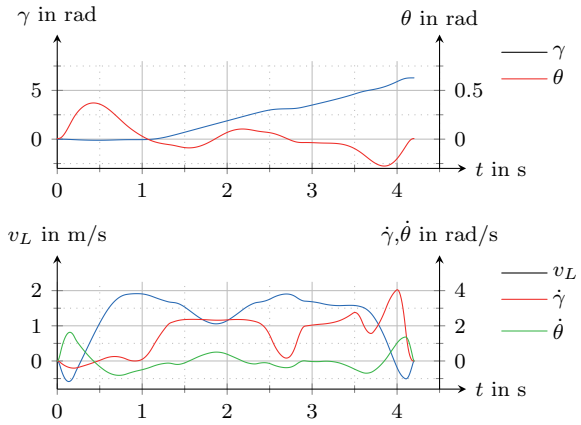

Fig. 3. Example Trajectory: State coordinates

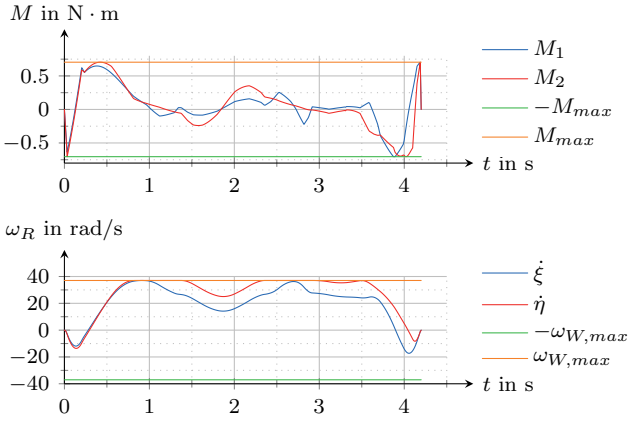

Fig. 4. Example Trajectory: Motor torque and wheel speed

form of the control system associated to a Segway model exhibits a strict feedforward structure. A constrained optimal control problem for energy/time optimal trajectory planning has been formulated. It is shown how the strict feedforward structure can be exploited for solving this problem with reduced computational effort. Simulation results are shown when the Segway is required to perform motion on a closed path within a predefined area. The calculated control torques can be used as feedforward within a model-based controller. This is a particularly important result since, so far, the Segway model could not been shown to be flat, and no flatness-based control method be applied. The optimal trajectories are currently being implemented on a real prototype. Future research will focus on identification of dynamic model parameters.

REFERENCES

Albert, K., Phogat, K.S., Anhalt, F., Banavar, R.N., Chatterjee, D., and Lohmann, B. (2018). Structure-preserving constrained optimal trajectory planning of a wheeled inverted pendulum.

Bremer, H. (2008). *Elastic Multibody Dynamics: A Direct Ritz Approach*. Springer Netherlands.

Cui, R., Guo, J., and Mao, Z. (2015). Adaptive backstepping control of wheeled inverted pendulums models. *Nonlinear Dynamics*, 79(1), 501–511.

Ghaffari, A., Shariati, A., and Shamekhi, A.H. (2016). A modified dynamical formulation for two-wheeled self-balancing robots. *Nonlinear Dynamics*, 83(1), 217–230.

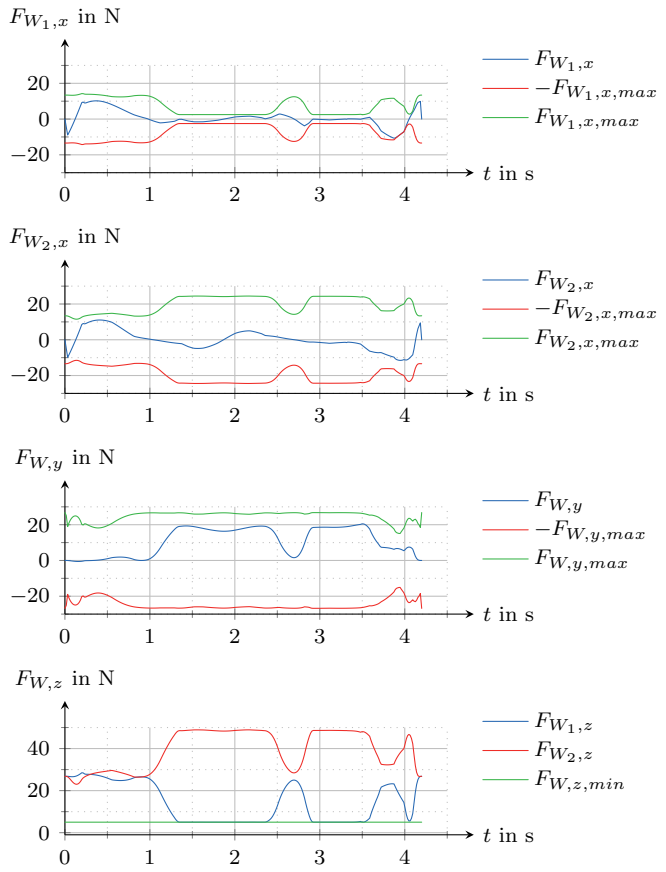

Fig. 5. Example Trajectory: Ground reaction forces

Isidori, A. (1995). *Nonlinear Control Systems*. Springer.

Kim, S. and Kwon, S. (2017). Nonlinear optimal control design for underactuated two-wheeled inverted pendulum mobile platform. *IEEE/ASME Transactions on Mechatronics*, 22(6), 2803–2808.

Kim, Y., Kim, S.H., and Kwak, Y.K. (2005). Dynamic analysis of a nonholonomic two-wheeled inverted pendulum robot. *Journal of Intelligent and Robotic Systems*, 44(1), 25–46.

Levine, J. (2009). *Analysis and control of nonlinear systems: A flatness-based approach*. Mathematical Engineering. Springer Berlin Heidelberg.

Pathak, K., Franch, J., and Agrawal, S.K. (2005). Velocity and position control of a wheeled inverted pendulum by partial feedback linearization. *IEEE Transactions on Robotics*, 21(3), 505–513.

Piegl, L. and Tiller, W. (2012). *The NURBS Book*. Springer Berlin Heidelberg.

Salerno, A. and Angeles, J. (2004). The control of semi-autonomous two-wheeled robots undergoing large payload-variations. In *IEEE International Conference on Robotics and Automation*, volume 2, 1740–1745.

Tall, I.A. and Respondek, W. (2005). Smooth and analytic normal and canonical forms for strict feedforward systems. In *Proceedings of the 44th IEEE Conference on Decision and Control*, 4213–4218.

Appendix A. EQUATIONS OF MOTION

For the representation of vectors in $\mathbb{R}^3$ the reference frames I, R and B are defined in Fig. 1. The rotation matrices

$$\mathbf{R}_{IR} = \begin{bmatrix} \cos(\gamma) & \sin(\gamma) & 0 \\ -\sin(\gamma) & \cos(\gamma) & 0 \\ 0 & 0 & 1 \end{bmatrix}, \quad \mathbf{R}_{RB} = \begin{bmatrix} \cos(\theta) & 0 & -\sin(\theta) \\ 0 & 1 & 0 \\ \sin(\theta) & 0 & \cos(\theta) \end{bmatrix}$$

transform from the R to the I reference frame and from the B to the R reference frame respectively. The absolute angular velocities of these reference frames are given by ${}_R\boldsymbol{\omega}_{IR} = (0\ 0\ \dot{\gamma})^\intercal$ and ${}_R\boldsymbol{\omega}_{IB} = \begin{pmatrix} 0 & \dot{\theta} & \dot{\gamma} \end{pmatrix}^\intercal$. The left index ${}_R(\cdot)$ indicates representation in frame R. The angular velocities of the three bodies are

$${}_B\boldsymbol{\omega}_{IB} = \mathbf{R}_{RB}{}^\intercal {}_R\boldsymbol{\omega}_{IB}, \quad {}_R\boldsymbol{\omega}_{IW_1} = \begin{pmatrix} 0 & \frac{2}{D_W}\left(v_L - \dot{\gamma} a_W\right) & \dot{\gamma} \end{pmatrix}^\intercal,$$

$${}_R\boldsymbol{\omega}_{IW_2} = \begin{pmatrix} 0 & \frac{2}{D_W}\left(v_L + \dot{\gamma} a_W\right) & \dot{\gamma} \end{pmatrix}^\intercal.$$

With the velocity vectors for the COM of the bodies

$${}_B\mathbf{v}_{C_B} = \begin{pmatrix} v_L \cos(\theta) + \dot{\theta} c_{B_z} \\ \dot{\gamma}\left(\cos(\theta) c_{B_x} + \sin(\theta) c_{B_z}\right) \\ v_L \sin(\theta) - \dot{\theta} c_{B_x} \end{pmatrix},$$

$${}_R\mathbf{v}_{C_{W_1}} = \begin{pmatrix} v_L - \dot{\gamma} c_{W_y} & 0 & 0 \end{pmatrix}^\intercal, \quad {}_R\mathbf{v}_{C_{W_2}} = \begin{pmatrix} v_L + \dot{\gamma} c_{W_y} & 0 & 0 \end{pmatrix}^\intercal$$

the momentum vectors are given by ${}_B\mathbf{p}_{C_B} = m_B {}_B\mathbf{v}_{C_B}$, ${}_R\mathbf{p}_{C_{W_1}} = m_W {}_R\mathbf{v}_{C_{W_1}}$ and ${}_R\mathbf{p}_{C_{W_2}} = m_W {}_R\mathbf{v}_{C_{W_1}}$. The angular momentum vectors are defined by

$$\begin{aligned} {}_B\mathbf{L}_{C_B} &= \operatorname{diag}\left(J_{B_x}, J_{B_y}, J_{B_z}\right) {}_B\boldsymbol{\omega}_{IB} \\ {}_R\mathbf{L}_{C_{W_1}} &= \operatorname{diag}\left(J_{W_r}, J_{W_a} + i_G{}^2 J_M, J_{W_r}\right) {}_R\boldsymbol{\omega}_{IW_1} \\ {}_R\mathbf{L}_{C_{W_2}} &= \operatorname{diag}\left(J_{W_r}, J_{W_a} + i_G{}^2 J_M, J_{W_r}\right) {}_R\boldsymbol{\omega}_{IW_2}. \end{aligned}$$

The forces due to gravity are ${}_B\mathbf{f}^e_{C_B} = \mathbf{R}_{RB}{}^\intercal \begin{pmatrix} 0 & 0 & -m_B g \end{pmatrix}^\intercal$ and ${}_R\mathbf{f}^e_{C_{W_1}} = {}_R\mathbf{f}^e_{C_{W_2}} = \begin{pmatrix} 0 & 0 & -m_W g \end{pmatrix}^\intercal$ and the torques due to the motors and viscous friction are

$${}_R\mathbf{M}^e_{C_{W_1}} = \begin{pmatrix} 0 \\ M_1 - d_1\left(\frac{2}{D_W}\left(v_L - \dot{\gamma} a_W\right) - \dot{\theta}\right) \\ 0 \end{pmatrix}$$

$${}_R\mathbf{M}^e_{C_{W_2}} = \begin{pmatrix} 0 \\ M_2 - d_2\left(\frac{2}{D_W}\left(v_L + \dot{\gamma} a_W\right) - \dot{\theta}\right) \\ 0 \end{pmatrix}$$

$${}_B\mathbf{M}^e_{C_B} = \mathbf{R}_{RB}{}^\intercal\left(-{}_R\mathbf{M}^e_{C_{W_1}} - {}_R\mathbf{M}^e_{C_{W_2}}\right).$$

The reaction forces/torques for base and wheel $i \in \{1, 2\}$

$$\begin{aligned} {}_B\mathbf{f}^z_{C_B} &= {}_B\dot{\mathbf{p}}_{C_B} + {}_B\tilde{\boldsymbol{\omega}}_{IB}\, {}_B\mathbf{p}_{C_B} - {}_B\mathbf{f}^e_{C_B} \\ {}_B\mathbf{M}^z_{C_B} &= {}_B\dot{\mathbf{L}}_{C_B} + {}_B\tilde{\boldsymbol{\omega}}_{IB}\, {}_B\mathbf{L}_{C_B} - {}_B\mathbf{M}^e_{C_B} \\ {}_R\mathbf{f}^z_{C_{W_i}} &= {}_R\dot{\mathbf{p}}_{C_{W_i}} + {}_R\tilde{\boldsymbol{\omega}}_{IR}\, {}_R\mathbf{p}_{C_{W_i}} - {}_R\mathbf{f}^e_{C_{W_i}} \\ {}_R\mathbf{M}^z_{C_{W_i}} &= {}_R\dot{\mathbf{L}}_{C_{W_i}} + {}_R\tilde{\boldsymbol{\omega}}_{IR}\, {}_R\mathbf{L}_{C_{W_i}} - {}_R\mathbf{M}^e_{C_{W_i}}. \end{aligned}$$

The EOM are then determined as (Bremer (2008))

$$\mathbf{0} = \begin{bmatrix} {}_B\mathbf{J}_{C_B}{}^\intercal & {}_R\mathbf{J}_{C_{W_1}}{}^\intercal & {}_R\mathbf{J}_{C_{W_2}}{}^\intercal \end{bmatrix} \begin{pmatrix} {}_B\mathbf{f}^z_{C_B} \\ {}_B\mathbf{M}^z_{C_B} \\ {}_R\mathbf{f}^z_{C_{W_1}} \\ {}_R\mathbf{M}^z_{C_{W_1}} \\ {}_R\mathbf{f}^z_{C_{W_2}} \\ {}_R\mathbf{M}^z_{C_{W_2}} \end{pmatrix}$$

with the Jacobian matrices

$${}_B\mathbf{J}_{C_B} = \begin{bmatrix} \frac{\partial\, {}_B\mathbf{v}_{C_B}}{\partial \dot{\mathbf{s}}} \\ \frac{\partial\, {}_B\boldsymbol{\omega}_{IB}}{\partial \dot{\mathbf{s}}} \end{bmatrix}, \qquad {}_R\mathbf{J}_{C_{W_i}} = \begin{bmatrix} \frac{\partial\, {}_R\mathbf{v}_{C_{W_i}}}{\partial \dot{\mathbf{s}}} \\ \frac{\partial\, {}_R\boldsymbol{\omega}_{IW_i}}{\partial \dot{\mathbf{s}}} \end{bmatrix}.$$

The EOM always train the form

$$\mathbf{M}(\theta)\ddot{\mathbf{s}} + \mathbf{g}(\theta, \dot{\mathbf{s}}) = \mathbf{B}\mathbf{u}.$$